

Covalent bonding and hybridization effects in the corundum-type transition-metal oxides V_2O_3 and Ti_2O_3

V. EYERT (*), U. SCHWINGENSCHLÖGL and U. ECKERN

Institut für Physik, Universität Augsburg, 86135 Augsburg, Germany

PACS. 71.20.-b – Electron density of states and band structure of crystalline solids.

PACS. 71.27.+a – Strongly correlated electron systems; heavy fermions.

PACS. 71.30.+h – Metal-insulator transitions and other electronic transitions.

Abstract. – The electronic structure of the corundum-type transition-metal oxides V_2O_3 and Ti_2O_3 is studied by means of the augmented spherical wave method, based on density-functional theory and the local density approximation. Comparing the results for the vanadate and the titanate allows us to understand the peculiar shape of the metal $3d$ a_{1g} density of states, which is present in both compounds. The a_{1g} states are subject to pronounced bonding-antibonding splitting due to metal-metal overlap along the c -axis of the corundum structure. However, the corresponding partial density of states is strongly asymmetric with considerably more weight on the high energy branch. We argue that this asymmetry is due to an unexpected broadening of the bonding a_{1g} states, which is caused by hybridization with the e_g^π bands. In contrast, the antibonding a_{1g} states display no such hybridization and form a sharp peak. Our results shed new light on the role of the a_{1g} orbitals for the metal-insulator transitions of V_2O_3 . In particular, due to a_{1g} - e_g^π hybridization, an interpretation in terms of molecular orbital singlet states on the metal-metal pairs along the c -axis is not an adequate description.

Based on the electronic level scheme of Castellani *et al.* [1], V_2O_3 was studied extensively as the canonical Mott–Hubbard system. Due to octahedral coordination of the metal sites, the V $3d$ states are split into lower t_{2g} and higher e_g^σ levels. Trigonal lattice symmetry leads to further separation of the former into a_{1g} and e_g^π states. Covalent V-V bonding along the hexagonal c -axis of the corundum structure results in bonding and antibonding a_{1g} molecular orbitals, which sort of bracket the e_g^π levels. Electronic structure calculations confirmed the gross features of this scheme with t_{2g} states close to the Fermi level [2]. As proposed by Castellani *et al.*, the bonding a_{1g} states are fully occupied, whereas the antibonding states shift to higher energies. This leaves one electron per V atom in the twofold degenerate e_g^π orbital and leads to an $S = 1/2$ state, suggesting to use the one-band Hubbard model at half filling for describing the metal-insulator transitions (MITs) of V_2O_3 . The stoichiometric compound undergoes an MIT at 168 K, leading from a paramagnetic metallic (PM) to an antiferromagnetic insulating (AFI) phase; on doping with Cr or Al a paramagnetic insulating (PI) phase is found [3, 4].

The model by Castellani *et al.* has been called into question by polarized x-ray absorption spectroscopy experiments, which point at an $S = 1$ spin state of the metal atoms [5]. The

(*) E-mail: volker.eyert@physik.uni-augsburg.de

lowest excited states miss pure e_g^π symmetry but reveal remarkable a_{1g} admixtures calling for a treatment beyond the one-band Hubbard model. LDA+U calculations explain the peculiar antiferromagnetic order at low temperatures and point at an $S = 1$ configuration [6], which also results from the model calculations by Mila *et al.* [7]. Starting with the assumption of strong covalent bonding in the V-V pairs parallel to the c -axis, these authors suppose the intersite a_{1g} hopping matrix element to dominate. However, a recent study of the hopping processes in V_2O_3 found relevant matrix elements also between second, third, and fourth nearest neighbours [8]. LDA band structures show only minor response to the structural modifications occurring at the phase transitions of V_2O_3 , whereas a correct description of the PM-PI transition has been obtained by a combination of LDA calculations with the dynamical mean field theory (DMFT) [9, 10]. Nonetheless, confirming an early suggestion by Dernier [11] we have recently demonstrated that considering the rearrangements of the metal-metal overlap *perpendicular* to the hexagonal c -axis is important for understanding the MITs of V_2O_3 [12–14].

Ti_2O_3 is isostructural to corundum V_2O_3 and undergoes a gradual MIT without symmetry breaking lattice distortion between 400 K and 600 K. In contrast to V_2O_3 , its low temperature insulating state is non-magnetic. As in V_2O_3 , the a_{1g} states mediate strong bonding between Ti-Ti pairs in face-sharing octahedra parallel to the hexagonal c -axis, leading to bonding and antibonding a_{1g} bands bracketing the e_g^π states. An insulating energy gap is expected between the bonding a_{1g} and e_g^π states [15]. According to this picture increase of the c/a ratio of the corundum lattice constants with increasing temperature reduces the a_{1g} band splitting and promotes a collapse of the energy gap. Band structure calculations by Mattheiss [16] revealed a partially filled t_{2g} complex of overlapping a_{1g} and e_g^π bands at the Fermi level. Decreasing the c/a ratio reduces but does not eliminate the a_{1g} - e_g^π band overlap. To open the gap, an unphysically small Ti-Ti distance of 2.2 Å parallel to the c -axis is required, which precludes a simple band explanation of the MIT. Recent cluster LDA+DMFT calculations assuming moderate Coulomb interactions among the t_{2g} orbitals reproduced the insulating state [17].

In this Letter we report on electronic structure calculations for both V_2O_3 and Ti_2O_3 using the respective room-temperature crystal structure data. Our calculations i) result in a new interpretation of the bonding and antibonding a_{1g} states and ii) reveal striking differences in the hybridizations of the V $3d$ e_g^π bands with the bonding and antibonding a_{1g} states, respectively. While hybridization of the e_g^π bands with the bonding a_{1g} states is rather strong, leading to significant broadening of these bands, the antibonding states are of pure a_{1g} character.

The present LDA band structure calculations are based on the scalar-relativistic augmented spherical wave (ASW) method [18, 19]. Crystallographic data reported by Dernier for V_2O_3 [11] and by Rice and Robinson for Ti_2O_3 [20] were used. To model the crystal potential in the large voids of the open crystal structures, additional augmentation spheres were included. Optimal augmentation sphere positions and radii of all spheres were automatically generated by the sphere geometry optimization (SGO) algorithm [21]. The basis sets comprised V/Ti $4s$, $4p$, $3d$, and O $2s$, $2p$ orbitals as well as states of the additional augmentation spheres. Brillouin zone integrations were performed using up to 2480 \mathbf{k} -points within the irreducible wedge.

As is typical for transition-metal chalcogenides with octahedral coordination, V_2O_3 shows three groups of bands in the vicinity of the Fermi level, extending from -8.8 eV to -3.9 eV, from -1.1 eV to 1.5 eV, and from 1.9 eV to 3.8 eV, see Fig. 1. They originate from O $2p$, V $3d$ t_{2g} , and V $3d$ e_g^σ states, respectively. The right hand side of Fig. 1 shows the V $3d$ density of states (DOS) for the latter two groups of bands separated into its symmetry components

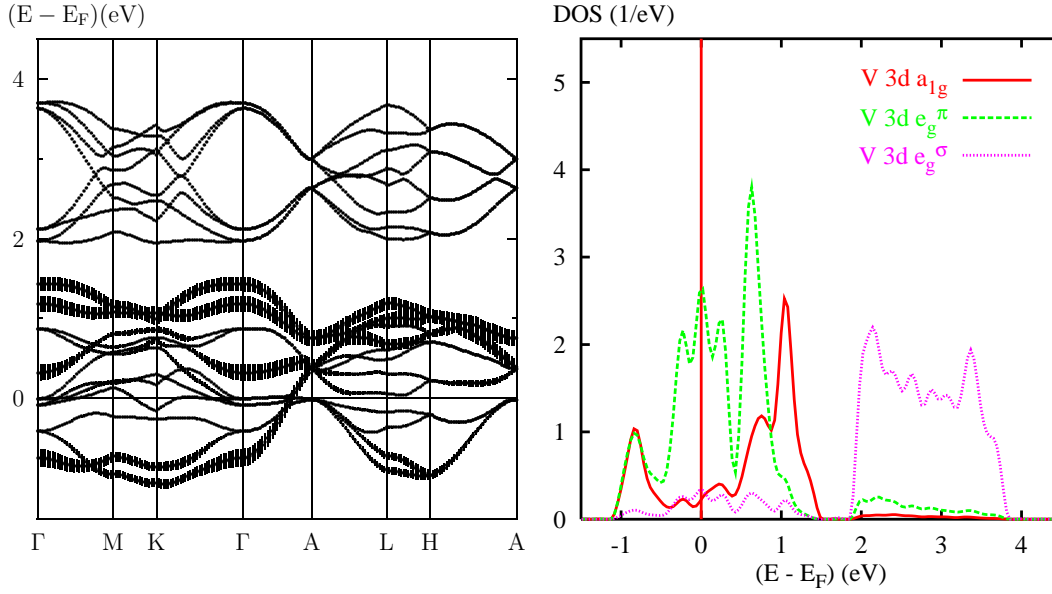


Fig. 1 – V_2O_3 : weighted electronic bands and partial V 3d DOS. The length of the bars in the band structure indicates V 3d a_{1g} contributions.

a_{1g} , e_g^π , and e_g^σ . V-O hybridization results in additional O 2p admixtures in the energy range shown, which are stronger for the σ -bonding e_g^σ states. Octahedral coordination of the metal atoms leads to almost perfect energetical separation of the t_{2g} and e_g^σ groups of bands. Small contributions of t_{2g} states in the e_g^σ energy range above 1.9 eV are mainly due to the V-V anti-dimerization along the c -axis, which shifts the metal atoms off the centers of their oxygen octahedra and results in a metal-metal distance much larger than the ideal value of $1/6$ of the c lattice constant.

The band structure of the t_{2g} and e_g^σ groups of bands is displayed on the left hand side of Fig. 1, where the length of the bars added to the bands is proportional to the respective a_{1g} contribution. Hence, bands without bars are of e_g^π and e_g^σ character, respectively, in the lower and upper group shown. The band structure refers to the non-primitive hexagonal representation of the trigonal unit cell. While the dispersion of the e_g^π bands is rather isotropic, the a_{1g} bands have an increased dispersion along the line Γ -A. Perpendicular to this line, i.e. along the paths Γ -M-K- Γ and A-L-H-A, the a_{1g} states are found mainly at the lower and upper boarder of the band complex at the Fermi level. This holds especially for the bands above 1 eV in the Γ -M-K- Γ plane, which are well separated from the lower lying bands.

The pronounced one-dimensionality of the a_{1g} bands leads to the characteristic shape of the a_{1g} partial DOS. It suggests to interpret the peak at -0.9 eV and the double-peak at $0.8/1.0$ eV, respectively, as the bonding and antibonding states resulting from the V-V overlap across the octahedral faces. However, the weights of these peaks are far from equal but have a ratio of about 1:3, contradicting expectations based on a molecular orbital point of view. Due to the reduced weight of the lower a_{1g} peak the occupation of the twofold degenerate e_g^π states is larger than one, explaining the experimental findings of Park *et al.* [5].

In order to understand these puzzling results we turn to titanium sesquioxide, which has the same octahedral coordination of the transition-metal sites with octahedra neighbouring

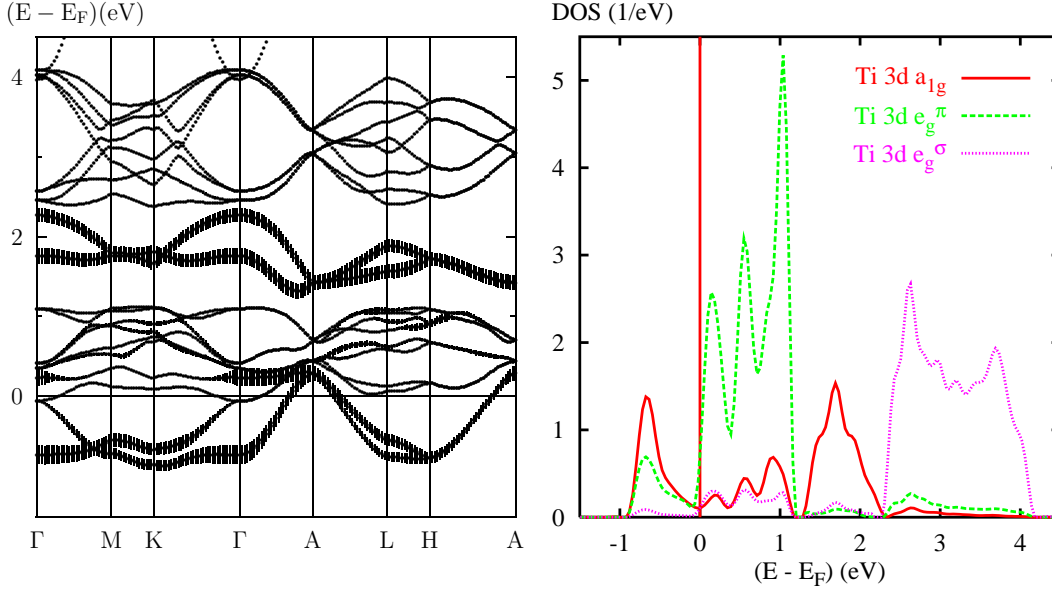


Fig. 2 – Ti_2O_3 : weighted electronic bands and partial Ti 3d DOS. The length of the bars in the band structure indicates Ti 3d a_{1g} contributions.

along the c -axis interlinked via faces. The band structure and the partial densities of states of Ti_2O_3 are displayed in Fig. 2, in the representation already used for V_2O_3 in Fig. 1. From the structural similarity of the two compounds we expect the same gross features of their electronic structures. Indeed, we obtain for Ti_2O_3 three groups of bands in the vicinity of the Fermi level, extending from -9.0 eV to -4.5 eV (O $2p$), -0.9 eV to 2.3 eV (Ti $3d\ t_{2g}$), and 2.4 eV to 4.1 eV (Ti $3d\ e_g^\sigma$). Additional Ti $4s$ bands are found at energies higher than 3.9 eV . These results agree well with the findings of Mattheiss [16].

The symmetry components of the Ti 3d DOS (right hand side of Fig. 2) confirm the energetical separation of the t_{2g} and e_g^σ states as well as the t_{2g} admixture to the bands above 2.4 eV due to the metal-metal anti-dimerization along the c -axis. In the band structure shown on the left hand side of Fig. 2 we distinguish the isotropically dispersing e_g^π bands from the a_{1g} states, which are highlighted by the bars attached to each band and display a rather one-dimensional behaviour. The latter causes the characteristic shape of the a_{1g} partial DOS with the pronounced peaks at -0.7 eV and 1.7 eV , which as before might be attributed to bonding-antibonding splitting due to metal-metal overlap along the c -axis. Yet, we are again faced with a decreased weight of the low-energy peak leading to the finite e_g^π occupation.

While the results for V_2O_3 and Ti_2O_3 are quite similar in general, we observe distinct differences at a closer look. They might give a first clue to the problem of the unequal weights of the a_{1g} peaks and pave the way for a better understanding of the role of these electronic states. To be specific, we point to the small gap at 1.2 eV in the partial DOS of the titanate, separating the peak at 1.7 eV from the lower lying bands. Such a gap is not observed for the vanadate. Since the a_{1g} partial densities of states both below and above 1.2 eV integrate to about one electron each, it is tempting to interpret the bands above this gap as antibonding and the whole of the a_{1g} bands between -1 eV and 1.2 eV as bonding. If this point of view were correct, the bonding a_{1g} states would thus extend over a very broad energy interval of

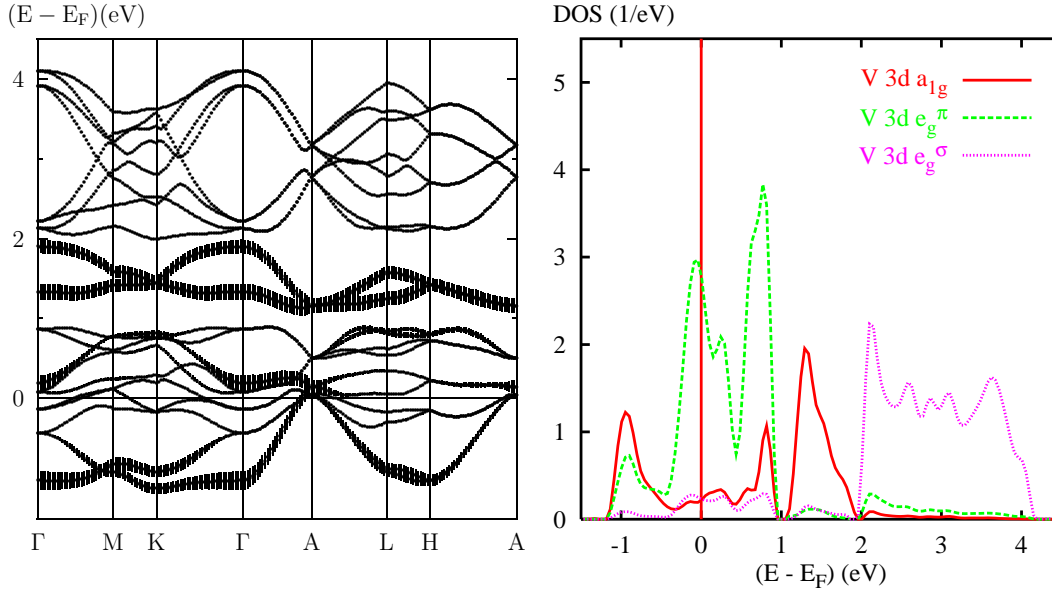


Fig. 3 – Hypothetical V_2O_3 (V-V bond lengths along c_{hex} compressed to 2.51 Å): weighted electronic bands and partial V 3d DOS. The length of the bars in the band structure indicates V 3d a_{1g} contributions.

more than 2 eV.

This quite unusual situation should be related to the second observation growing out of the comparison of Figs. 1 and 2, namely the conspicuous downshift of the upper edge of the e_g^π states. While in the vanadate these bands share edges with the whole of the a_{1g} states, there exists only a tiny contribution at energies above 1.2 eV in the titanate. In contrast, the e_g^π partial DOS displays a very sharp cutoff at this energy. Obviously, the e_g^π states are found only in the energy region of the bonding but not of the antibonding a_{1g} states. Going one step further, we infer from the similar shape of both partial densities of states below 1.2 eV, in particular from the common peaks near -0.7 eV, 0.2 eV, 0.5 eV, and 1.0 eV, a considerable amount of a_{1g} - e_g^π mixing. We thus attribute the large band width of the low-energy a_{1g} states to the strong a_{1g} - e_g^π hybridization. Since the broadening is of similar size as the bonding-antibonding splitting of the a_{1g} band, we end up with the complex situation observed for the vanadate.

In order to “prove” the just sketched scenario, we turn in the last step to another set of calculations for V_2O_3 with a hypothetical crystal structure. In this structure the V-V bond length along the c -axis has been reduced from 2.70 Å to 2.51 Å, while the symmetry of the corundum structure, the lattice constants, and the oxygen positions were retained. As a result of these changes, hypothetical V_2O_3 is characterized by a short intrapair V-V distance, hence, by increased intrapair bonding. Eventually, this will cause a stronger bonding-antibonding splitting of the a_{1g} states. As a consequence, we expect a much clearer separation of these states as compared to the results given in Fig. 1. The band shifts occurring on going from the real to the artificial structure of V_2O_3 will thus allow us to make a clear distinction between bonding and antibonding a_{1g} states for this material.

The calculated results for the hypothetical V_2O_3 structure are displayed in Fig. 3, using the same representation of the band structure and V 3d DOS as in Figs. 1 and 2. While the

V $3d$ e_g^σ DOS of artificial V_2O_3 still resembles the results for real V_2O_3 , we observe indeed distinct modifications especially for the a_{1g} DOS. The peak at -0.8 eV in Fig. 1 shifts to lower energies, and the peak at 1.0 eV (having a pronounced shoulder at 0.7 eV, see Fig. 1) splits into two peaks at 0.8 eV and 1.3 eV leaving a gap at about 1.0 eV. At the same time the upper edge of the e_g^π states experiences a strong downshift and displays a sharp cutoff. Eventually, the band structures and densities of states of artificial V_2O_3 become more similar to those of Ti_2O_3 . From the differences between real and artificial V_2O_3 we thus associate the a_{1g} peak around 1.3 eV with the antibonding states due to intrapair bonding. At lower energies, strong a_{1g} - e_g^π hybridization leads to a considerable broadening of the bonding a_{1g} branch, which extends from -1.2 eV to 1.0 eV. Note that both the bonding and antibonding states integrate to equal weights. Transferring these findings to real V_2O_3 , we conclude that the a_{1g} peak at 1.0 eV in Fig. 1 represents the antibonding states, whereas the region of bonding states extends from -1.1 eV to ≈ 0.9 eV and even includes the shoulder at 0.7 eV.

In general, our findings agree well with the results of the recent LDA+U calculations by Ezhov *et al.* as well as Elfimov *et al.* for antiferromagnetic and assumed ferromagnetic V_2O_3 [6,8]. The main difference between both approaches concerns the relative downshift of the e_g^π states, which eventually opens the insulating gap observed for the AFI phase. However, the LDA+U calculations likewise result in a finite a_{1g} - e_g^π hybridization for the bonding a_{1g} states whereas the e_g^π admixture to the antibonding a_{1g} states vanishes. Hence, while the LDA+U treatment leads to a somewhat changed scenario the basic mechanisms are still well described by the LDA calculations.

Still, it remains an open question why the bonding a_{1g} states are subject to hybridization with the e_g^π states, while the antibonding states retain their pure band character. Of course, it is tempting to relate this finding to the aforementioned metal-metal anti-dimerization, which shifts the metal atoms along the c -axis off the center of their respective oxygen octahedra. Since the displacement is parallel to the principal axis of the a_{1g} orbitals, the resulting increase in d - p overlap mainly affects these states and is much less pronounced for the e_g^π bands. The a_{1g} states are thus found at slightly elevated energy, the difference of the centers of gravity amounting to ≈ 0.3 eV for V_2O_3 [10]. As a consequence, the lower bonding part of the a_{1g} bands experiences more overlap with the e_g^π states than the high-energy antibonding a_{1g} states.

Nevertheless, a more convincing argument is based on the symmetry of the electronic orbitals involved, as well as the much different degree of overlap of the t_{2g} orbitals within the c -axis pairs. As a matter of fact, the e_g^π orbitals arise as linear combinations of all five d states, except for the $d_{3z^2-r^2}$ states which are identical to the a_{1g} states. In addition, the overlap of the e_g^π orbitals within the vanadium pairs along the c -axis is close to negligible. As a consequence, these states are symmetric with respect to reflection about the midplane between the two atoms. This is different for the a_{1g} states, which do overlap along the c -axis this leading to the bonding and antibonding combinations. Since the bonding and antibonding a_{1g} states are even and odd functions with respect to reflections, only the former may hybridize with the e_g^π orbitals, whereas the latter do not overlap with these states.

In conclusion, the electronic structure of the corundum-type sesquioxides V_2O_3 and Ti_2O_3 is strongly influenced by a complex interplay of i) the formation of bonding and antibonding states arising from overlap of the metal $3d$ a_{1g} states across octahedral faces and ii) strong hybridization of the bonding but not the antibonding a_{1g} bands with the e_g^π states. The hybridization disturbs the formation of molecular orbital singlet states by the a_{1g} orbitals of the vertical V-V pairs. Therefore, the occupation of the e_g^π bands is increased this explaining the recently observed $S = 1$ configuration. As a consequence, failure of the model by Castellani *et al.* is mainly due to hybridization effects and not purely a consequence of the energy lowering of the e_g^π states. In addition, since for symmetry reasons the a_{1g} - e_g^π hybridization affects only

the bonding a_{1g} states, the corresponding partial DOS assumes a strongly asymmetric shape. The observed strong 3D-coupling of the a_{1g} orbitals appears to be a primal feature of the electronic structure of these sesquioxides and therefore is of special importance for models dealing with the MITs in this compound. The findings for V_2O_3 strongly differ from those for VO_2 and Ti_4O_7 , where hybridization between the $d_{||}$ states, which are responsible for metal-metal overlap, and the e_g^π states is suppressed and thus allows for a Peierls-type mechanism of the MIT [22, 23].

* * *

This work was supported by the Deutsche Forschungsgemeinschaft (DFG) through Sonderforschungsbereich 484.

REFERENCES

- [1] CASTELLANI C., NATOLI C. R. and RANNINGER J., *Phys. Rev. B*, **18** (1978) 4945; **18** (1978) 4967; **18** (1978) 5001.
- [2] MATTHEISS L. F., *J. Phys.: Condens. Matter*, **6** (1994) 6477.
- [3] MCWHAN D. B., REMEIK A. J. P., RICE T. M., BRINKMAN W. F., MAITA J. P. and MENTH A., *Phys. Rev. Lett.*, **27** (1971) 941.
- [4] MCWHAN D. B., MENTH A., REMEIK A. J. P., BRINKMAN W. F. and RICE T. M., *Phys. Rev. B*, **7** (1973) 1920.
- [5] PARK J.-H., TJENG L. H., TANAKA A., ALLEN J. W., CHEN C. T., METCALF P., HONIG J. M., DE GROOT F. M. F. and SAWATZKY G. A., *Phys. Rev. B*, **61** (2000) 11506.
- [6] EZHOV S. YU., ANISIMOV V. I., KHOMSKII D. I. and SAWATZKY G. A., *Phys. Rev. Lett.*, **83** (1999) 4136.
- [7] MILA F., SHIINA R., ZHANG F.-C., JOSHI A., MA M., ANISIMOV V. and RICE T. M., *Phys. Rev. Lett.*, **85** (2000) 1714.
- [8] ELFIMOV I. S., SAHA-DASGUPTA T. and KOROTIN M. A., *Phys. Rev. B*, **68** (2003) 113105.
- [9] HELD K., KELLER G., EYERT V., VOLLHARDT D. and ANISIMOV V. I., *Phys. Rev. Lett.*, **86** (2001) 5345.
- [10] KELLER G., HELD K., EYERT V., VOLLHARDT D. and ANISIMOV V. I., *Phys. Rev. B*, **70** (2004) 205116.
- [11] DERNIER P. D., *J. Chem. Phys. Solids*, **31** (1970) 2569.
- [12] SCHWINGENSCHLÖGL U., EYERT V. and ECKERN U., *Europhys. Lett.*, **61** (2003) 361.
- [13] SCHWINGENSCHLÖGL U., EYERT V. and ECKERN U., *Europhys. Lett.*, **64** (2003) 682.
- [14] SCHWINGENSCHLÖGL U. and EYERT V., *Ann. Phys. (Leipzig)*, **13** (2004) 475.
- [15] VAN ZANDT L. L., HONIG J. M. and GOODENOUGH J. B., *J. Appl. Phys.*, **39** (1968) 594.
- [16] MATTHEISS L. F., *J. Phys.: Condens. Matter*, **8** (1996) 5987.
- [17] POTERYAEV A. I., LICHTENSTEIN A. I. and KOTLIAR G., *Phys. Rev. Lett.*, **93** (2004) 086401.
- [18] WILLIAMS A. R., KÜBLER J. and GELATT C. D. JR., *Phys. Rev. B*, **19** (1979) 6094.
- [19] EYERT V., *Int. J. Quant. Chem.*, **77** (2000) 1007.
- [20] RICE C. E. and ROBINSON W. R., *Acta Crystallogr. B*, **53** (1977) 1342.
- [21] EYERT V. and HÖCK K.-H., *Phys. Rev. B*, **57** (1998) 12727.
- [22] EYERT V., *Ann. Phys. (Leipzig)*, **11** (2002) 650.
- [23] EYERT V., SCHWINGENSCHLÖGL U., and ECKERN U., *Chem. Phys. Lett.*, **390** (2004) 151.